Toward higher order event–capturing schemes and adaptive time–step strategies for nonsmooth multibody systems

Vincent Acary

▶ **To cite this version:**

Vincent Acary. Toward higher order event–capturing schemes and adaptive time–step strategies for nonsmooth multibody systems. [Research Report] RR-7151, 2009, pp.31. inria-00440771v1

HAL Id: inria-00440771

https://inria.hal.science/inria-00440771v1

Submitted on 15 Dec 2009 (v1), last revised 25 Aug 2010 (v2)

HAL is a multi-disciplinary open access archive for the deposit and dissemination of scientific research documents, whether they are published or not. The documents may come from teaching and research institutions in France or abroad, or from public or private research centers.

L'archive ouverte pluridisciplinaire **HAL**, est destinée au dépôt et à la diffusion de documents scientifiques de niveau recherche, publiés ou non, émanant des établissements d'enseignement et de recherche français ou étrangers, des laboratoires publics ou privés.

INRIA

INSTITUT NATIONAL DE RECHERCHE EN INFORMATIQUE ET EN AUTOMATIQUE

Toward higher order event–capturing schemes and adaptive time–step strategies for nonsmooth multibody systems

Vincent Acary

N° 7151

December 14, 2009

Thème NUM

ISSN 0249-6399 ISRN INRIA/RR--7151--FR+ENG

INSTITUT NATIONAL
DE RECHERCHE
EN INFORMATIQUE
ET EN AUTOMATIQUE

INRIA

centre de recherche
GRENOBLE - RHÔNE-ALPES

Toward higher order event–capturing schemes and adaptive time–step strategies for nonsmooth multibody systems

Vincent Acary*

Thème NUM — Systèmes numériques
Équipe-Projet Bipop

Rapport de recherche n° 7151 — December 14, 2009 — 28 pages

Abstract: The report is devoted to the study of higher order time integration methods for multibody systems with unilateral constraints. After a brief presentation of the mathematical modelling of nonsmooth multibody systems, several estimates on the local error of consistency of the Moreau time–stepping scheme are given. Based on these estimates, an attempt at an adaptive time–step strategy is presented on academic examples. Finally, higher order event–capturing methods are designed by coupling implicit Runge–Kutta schemes and the Moreau's time–stepping scheme.

Key-words: Multibody systems, nonsmooth Mechanics, unilateral constraints, impact, Moreau's sweeping process, numerical integration scheme, Adaptive time–step strategy, order of accuracy, error estimates.

* vincent.acary@inrialpes.fr

Centre de recherche INRIA Grenoble – Rhône-Alpes
655, avenue de l'Europe, 38334 Montbonnot Saint Ismier
Téléphone : +33 4 76 61 52 00 — Télécopie +33 4 76 61 52 52

Vers des schémas à capture d'évévements d'ordre élevé et des stratégies de pas de temps adaptatif pour les systèmes multi–corps non–réguliers.

Résumé : Dans ce rapport, on s'intéresse à l'étude des schémas d'ordre élevé pour l'intégration en temps des systèmes multi–corps avec contraintes unilatérales. Après une brève présentation de la modélisation mathématique des systèmes multi–corps non réguliers, plusieurs estimations de l'erreur de consistance sont fournies. En se basant sur ces estimations, un essai de stratégie de pas de temps adaptatif est présenté sur des exemples académiques. Finalement, des schémas à capture d'événements sont développés en couplant des schémas de Runge–Kutta implicites et le schéma de Moreau.

Mots-clés : Systèmes multi–corps, Mécanique non régulière, contraintes unilatérales, impact Processus de rafle de Moreau, Schémas numériques d'intégration, pas de temps adaptatifs, ordre de précision, estimations d'erreurs.

Notation

The following notation is used throughout the paper. The uniform norm for a function f is denoted by $\|f\|_\infty$ and for a vector $x \in I\!R^n$ by $\|x\|$. The set of p-continuously differentiable mapping is $\mathcal{C}^p$. Let I a real time interval of any sort. The set of functions $f : I \to I\!R^n$ of bounded variations (BV) is denoted by $BV(I, I\!R^n)$. For $f \in BV(I, I\!R^n)$, we denote the right–limit function as $f^+(t) = \lim_{s\to t, s>t} f(s)$, and respectively the left–limit as $f^-(t) = \lim_{s\to t, s<t} f(s)$. We use the following convention introduced in Moreau [1988b]: if I contains its left end, T_l (respectively its right end T_r) we shall agree that $f^-(T_l) = f(T_l)$ (respectively $f^+(T_r) = f(T_r)$). The set of functions $f : I \to I\!R^n$ of Locally Bounded Variations (LBV) is denoted by $LBV(I, I\!R^n)$. We denote by $0 = t_0 < t_1 < \ldots < t_k < \ldots < t_N = T$ a finite partition (or a subdivision) of the time interval $[0, T]$ ($T > 0$). The integer N stands for the number of time intervals in the subdivision. The length of a time step is denoted by $h_k = t_{k+1} - t_k$. For simplicity sake, the schemes are presented in the sequel with a time step shortly denoted by h. The value of a real function $x(t)$ at the time t_k, is approximated by x_k. In the same way, the notation ($\theta \in [0, 1]$) $x_{k+\theta} = (1 - \theta)x_k + \theta x_{k+1}$ is used for $\theta \in [0, 1]$. The notation $\mathcal{O}(h)$ is to be understood as $h \to 0$. The notation dt defined the Lebesgue measure on $I\!R$.

1 Introduction and Motivations

In order to precise the motivation of this work, let us briefly recall what is the context of the modeling and the simulation of multibody systems with unilateral constraints. Let us consider a multibody systems described by a generalized coordinates vector $q(t) \in I\!R^n$ and a generalized velocities vector $v(t) \in I\!R^n$. In a pure Lagrangian setting, the equation of motion of the multibody systems with unilateral constraints may be written down as

$$\begin{cases} q(t_0) = q_0,\, v(t_0) = v_0 & \text{(1a)} \\ \dot{q}(t) = v(t), & \text{(1b)} \\ M(q(t))\dot{v}(t) + F(t, q(t), v(t)) = G(t, q)\lambda(t), & \text{(1c)} \\ g^\alpha(t, q(t)) = 0, \quad \alpha \in \mathcal{E}, & \text{(1d)} \\ g^\alpha(t, q(t)) \geqslant 0, \quad \lambda^\alpha \geqslant 0, \quad \lambda^\alpha g^\alpha(t, q) = 0 \quad alpha \in \mathcal{I}, & \text{(1e)} \end{cases}$$

where

- the initial conditions are $q_0 \in I\!R^n$ and $v_0 \in I\!R^n$,
- the mapping $M : I\!R^n \to I\!R^{n\times n}$ is the inertia matrix,
- the mapping $F : I\!R \times I\!R^n \times I\!R^n \to I\!R^n$ contains the external forces applied to the system, the internal forces and possibly the gyroscopic forces,
- the mapping $g : I\!R \times I\!R^n \to I\!R^m$ describes the constraints on the system, whose Jacobian is denoted by the mapping $G(t, q) : I\!R \times I\!R^n \to I\!R^{m\times n}$ that is $G(t, q) = \nabla_q g(t, q)$, and
- the set $\mathcal{E} \subset I\!N$ et $\mathcal{I} \subset I\!N$ respectively describe the set of bilateral constraints and unilateral constraints.

The choice of the Lagrangian setting rather than another formulation (e.g. Newton/Euler) is chosen for the sake of simplicity without any loss of generality for the further developments. Similarly, we will consider in this paper that $\mathcal{E} = \emptyset$ and that the constraints are holonomic constraints. The methods and results developed in this context extend straightforwardly to the more general case (1). Finally, let us define the following variables relative to constraints, called *local variables* the local velocity $U(t)$ and the (local) Lagrange multiplier $\lambda(t)$ which is associated with the generalized reaction forces $r(t)$ such that

$$U(t) = G^T(q)\, v(t), \qquad r(t) = G(q)\lambda(t). \tag{2}$$

By denoting $g(q) = [g_k(q), k \in \mathcal{I}]^T$ and $\lambda = [\lambda_k, k \in \mathcal{I}]^T$, the condition (1d) is called the *Signorini condition* or the complementarity condition which will denoted shortly as

$$0 \leqslant g(q) \perp \lambda \geqslant 0, \quad \text{or equivalently } -\lambda \in N_{\mathbb{R}^m_+}(g(q)). \tag{3}$$

The set $N_K(x)$ stands for the normal cone to a convex set K [Moreau, 1967, Rockafellar, 1970] taken at x. Using the inclusion in 3, the dynamics can be cast into an Differential Inclusion (DI) form as

$$\begin{cases} \dot{q}(t) = v(t), & \text{(4a)} \\ M(q(t))\dot{v}(t) + F(t, q(t), v(t)) = r(t) \in -G(q(t))\, N_{\mathbb{R}^m_+}(g(q(t))). & \text{(4b)} \end{cases}$$

It is well-know that such a dynamics can be nonsmooth and may encounter jumps in the velocities. Therefore, the velocity v usually belongs to $LBV(I, \mathbb{R}^n)$ and the acceleration as a differential measure $\mathrm{d}v$ associated with v. The absolutely continuous generalized coordinates q is integrated from the velocity in an usual way

$$q(t) = q(t_0) + \int_{t_0}^{t} v(\tau)\, d\tau, \tag{5}$$

and the dynamics (4) is reformulated as a Measure Differential Inclusion (MDI),

$$M(q(t))\, \mathrm{d}v - F(t, q(t), v^+(t))\, \mathrm{d}t = -G(q(t))\, N_{\mathbb{R}^m_+}(g(q(t))). \tag{6}$$

The Lagrange multiplier λ is then replaced by a measure $\mathrm{d}I$ such that

$$-\mathrm{d}I \in N_{\mathbb{R}^m_+}(g(q)). \tag{7}$$

and similarly at the generalized forces level r is replaced by $\mathrm{d}i = G(q)\mathrm{d}I$. To complete the modeling of a multibody system with unilateral constraints, an impact law has to be stated to define the value of the velocity after a jump. Without entering into deeper details of the impact modeling, the Newton impact law is chosen for its simplicity in order to define the post-impact velocity such that

$$U^+(t) = -eU^-(t). \tag{8}$$

where e is the coefficient of restitution.

For more details on the modeling of multibody systems with unilateral constraints, we refer to [Acary and Brogliato, 2008, Pfeiffer and Glocker, 1996, Moreau, 1988a] and for the mathematical analysis, we refer to [Schatzman, 1978, Monteiro Marques, 1993, Stewart, 2000, Ballard, 2000].

Remark 1 *Note that the formulation (6) encompasses the dynamics of flexible multi–body systems which are space–discretized by Finite Element Method (FEM) or any other Galerkin–type method. In the case of standard FEM applications, the generalized coordinates q are the displacements at the nodes of the mesh. In co–rotational approaches[Géradin and Cardona, 2001], the generalized coordinates are a mixture of finite rotations and displacements at the nodes of the mesh in a spatial frame (see [Brüls et al., 2008] for a comprehensive discussion).*

Throughout the paper, two test examples will be chosen to highlight the property of the considered numerical integration scheme.

Example 1 (The bouncing ball) *This is the standard bouncing ball under gravity depicted in Figure 1(a). The dynamics is constant with a forcing term equal to f together with an unilateral contact on the ground,*

$$\begin{cases} \dot{v}(t) = f(t) + \lambda(t), \qquad \dot{q}(t) = v(t), \\ 0 \leqslant q(t) \perp \lambda(t) \geqslant 0, \quad v^+(t) = -ev^-(t), \ \textit{if } q(t) = 0, \end{cases} \tag{9}$$

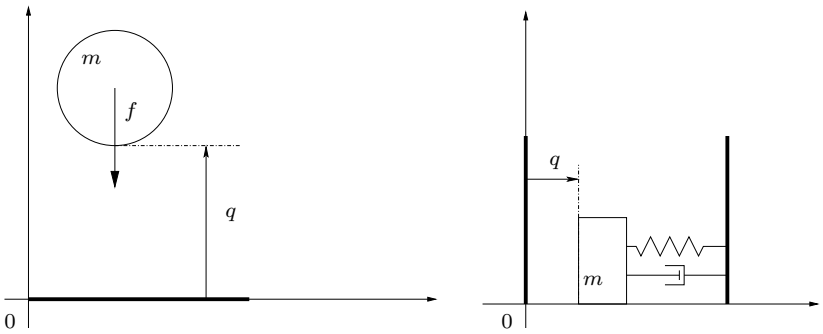

(a) The bouncing ball (b) The linear oscillator

Figure 1: Simple archetypal test examples

The interesting feature of the bouncing ball example is the presence of a finite accumulation of impact when $0 < e < 1$ *and* $f < 0$. *The analytical solution of this example can be found in [Brogliato, 1999]. We give here a more pleasant analytical solution due to Ballard [Ballard, 2003] which will be used as a benchmark in the further sections. The parameters are chosen as* $f = -2$, $e = 1/2$ *and the initial data as* $t_0 = 0, q_0 = 1$ *and* $v_0 = 0$. *The analytical solution reads*

$$\begin{cases} q(t) = -t^2 + 1, \\ v(t) = -2t, \end{cases} \qquad t \in [0, 1)$$

$$\begin{cases} q(t) = -(t-3)^2 - \dfrac{3}{2^n}(t-3) + \dfrac{1}{2^{n-1}}\left(3 - \dfrac{1}{2^n}\right), \\ v(t) = -2(t-3) - \dfrac{3}{2^n}, \end{cases} \qquad t \in \left[3 - \frac{1}{2^{n-1}}, 3 - \frac{1}{2^n}\right), \tag{10}$$

$$\begin{cases} q(t) = 0, \\ v(t) = 0, \end{cases} \qquad t \in [3, +\infty).$$

Example 2 (The linear oscillator example) *The dynamics of this one-degree-of-freedom system depicted in Figure 1(b) example is similar to the dynamics (9) but with a linear spring–damper internal force, that is*

$$m\dot{v}(t) + cv(t) + kq(t) = \lambda(t). \tag{11}$$

The previous trivial free dynamics (9) with a null or a constant forcing term are exactly integrated with any first order scheme. In the case of a linear dynamics, we can measure discrepancies between various numerical methods with various orders. The explicit analytical solution can be found in [Janin and Lamarque, 2001].

Two types of methods are currently available to numerically integrate in time the nonsmooth multibody systems. We briefly summarize their properties in the following paragraphs.

Nonsmooth event tracking method. These methods are also called *Event-driven* methods, where the time of discontinuities in the velocity or in its derivatives, also called an *nonsmooth event* or shortly an event, is detected and accurately located. Between two events, the system is integrated with any standard Differential Algebraic Equations (DAE) solver with a suitable order according to the regularity of the system. Such a method, detailed in [Pfeiffer and Glocker, 1996, Abadie, 2000, Acary and Brogliato, 2008] can be very efficient on several simple problems but suffers for several drawbacks. If the number of events is large or worth infinite, in a finite time interval, the time integration cannot efficiently advance in time. This is particularly the case when a finite accumulation is encountered. Secondly, in practice the method is very sensitive to numerical tolerances used in the detection procedure of events. Thirdly, such a method requires a reformulation of the constraints at higher kinematic levels (velocity, acceleration, ...). Due

to the intrinsic unilateral character of the constraints, the derivatives of the constraints involve some additional conditional statements. On the numerical point of view, this index-like reduction implies the introduction of new numerical tolerances to trigger the conditional statements and theirs associated difficulties. Shortly speaking, the event-driven approaches are well–suited when the nonsmooth events are rare and well-separated in time in small–scale nonsmooth multi–body systems.

Nonsmooth event capturing method These methods are also called shortly as *time–stepping methods*. The two main nonsmooth event capturing methods are due to Moreau [Moreau, 1988a] and to Paoli & Schatzman [Paoli and Schatzman, 2002a,b]. We have decided to focus our work on the Moreau time–stepping scheme mainly due to length restrictions. In such methods, the time-integration is performed with a time step, whose length does not depend on the exact location of nonsmooth events. The advantages of this class of methods are the convergence proofs, the efficiency even in the case of finite accumulation of impacts and the fact that are able to work without any accurate event detection. Finally, another practical interest of this method is that it does not require higher derivation of the unilateral constraints (velocity level for the Moreau scheme and direct coordinate level for the Schatzman–Paoli scheme). However, the major drawback of this method is its low order of accuracy. When events are encountered, the local error of consistency is at best $\mathcal{O}(h)$. On smooth phases, the order $\mathcal{O}(h^2)$ is expected as for the numerical integration of index-2 DAE with the backward Euler method.

The objective of this paper is to propose several alternative nonsmooth event capturing methods, *i.e.* time-stepping methods with higher–order accuracy results and better efficiency. The efficiency is measured by the ratio of the global error and the CPU effort. The targeted applications are the mechanical systems with a small number of bodies, but where unilateral contact and the free motion plays a important role of the global behavior of the system. The rigid multi-body systems in circuit breakers [Abadie, 2000], robotic and control applications [Acary et al., 2008, Herdt et al., 2009], automotive applications [Glocker et al., 2009] are the favorite ones. In such applications, the accurate treatment of large number of events and finite accumulation due to the proper dynamics or clearances in joints is crucial. The quest for high accuracy in large–scale systems such as granular materials or large scale finite element applications is very expensive and most of time useless. Nevertheless, the methods developed in this paper should apply to this type of systems but with an extreme CPU effort.

Finally, the work in [Studer et al., 2008, Studer, 2009] has to be cited as the first attempt to increase the efficiency of Moreau's scheme by an extrapolation method. However in this latter, no proofs of order of accuracy can be found and the authors made the assumption that Moreau's scheme has an order of accuracy equal to one. We will see that the assumption fails to be satisfied in most cases.

2 Moreau's sweeping process and time–stepping scheme

Moreau's scheme [Moreau, 1983, 1988a, 1999] for scleronomous holonomic perfect unilateral constraints is based on a formulation of the unilateral constraint in terms of local velocities together with the Newton impact law (see for details [Monteiro Marques, 1993, Ballard, 2000, Stewart, 1998]).

Moreau [Moreau, 1988a] proposed a compact formulation of the impact law as an MDI,

$$-\mathrm{d}I \in N_{T_{\mathbb{R}^m_+}(g(q(t)))}(U^+(t) + eU^-(t)) \tag{12}$$

where $T_{\mathbb{R}^m_+}(y)$ stands for the tangent cone to $\mathbb{R}^m_+$ at y [Moreau, 1967, Rockafellar, 1970]. Finally, we obtain an MDI, the so-called *Moreau sweeping process*,

$$M(q(t))\,\mathrm{d}v - F(t, q(t), v^+(t))\,\mathrm{d}t \in -G(q(t))N_{T_{\mathbb{R}^m_+}(y(t))}(U^-(t) + eU^-(t)). \tag{13}$$

Remark 2 *This formulation of the unilateral constraints together with Newton's impact law can be interpreted as an index reduction technique in DAE theory. In continuous time, the constraints on the generalized coordinates is also satisfied if it is satisfied in the initial conditions. In discrete time, it ensures the satisfaction of the Newton's impact law in discrete time and possesses very good stability properties such that the chattering free stabilization on the constraints in the nonsmooth multibody dynamics,.*

Well–posedness assumptions The following assumptions are made to ensure the well–posedness of the problem.

Assumption 1 (Existence and uniqueness) *A unique global solution over* $[0,T]$ *for the Moreau's sweeping process is assumed such that* $q(\cdot)$ *is absolutely continuous and admits a right velocity* $v^+(\cdot)$ *at every instant* t *of* $[0,T]$ *and such that the function* $v^+ \in LBV([0,T],\mathbb{R}^n)$.

Assumption 1 is ensured in the framework introduced by Ballard [Ballard, 2000] who proves the existence and uniqueness of a solution in a general framework mainly based on th analyticity of data. The further following assumption is made to ensure the consistent use of time–stepping scheme of order $p \geqslant 1$ in the smooth phases of the motion.

Assumption 2 (Smoothness of data) *The following smoothness on the data will be assumed: a) the inertia operator* $M(q)$ *is assumed to be of class* $\mathcal{C}^p$ *and definite positive, b) the force mapping* $F(t,q,v)$ *is assumed to be of class* $\mathcal{C}^p$*, c) the constraint functions* $g(q)$ *are assumed to be of class* $\mathcal{C}^{p+1}$ *and d) the Jacobian matrix* $G(q) = \nabla_q^T g(q)$ *is assumed to have full-row rank.*

Throughout the paper, the definition of a smooth phase is as follows

Definition 1 (Smooth phase of evolution) *Let us assume that the date satisfies Assumption 2. The system undergoes a smooth evolution over a so-called* smooth phase *denoted by* $S \subset I \subset \mathbb{R}$ *if the local velocity* $U^-(t) = U^+(t) \geqslant 0$ *for all* $t \in S$.

On a smooth phase, solving (1) amounts to solve an index-3 DAE. Under Assumption 2, an unique maximal solution of class $\mathcal{C}^{p+1}$ in the smooth phase is ensured [Ballard, 2000]. Under Assumption 2, the problem (13) can be stated in terms of the local variables U and $\mathrm{d}I$ such that

$$\begin{cases} \mathrm{d}U = W(q(t))\mathrm{d}I + G^T(q(t))M^{-1}(q(t))F(t,q(t),v^+(t)), \\ -\mathrm{d}I \in N_{T_{\mathbb{R}^m_+}(y(t))}(U^-(t) + eU^-(t)), \end{cases} \tag{14}$$

where $W(q) = G^T(q)M^{-1}(q)G(q)$ is called the *Delassus operator* which is also of class $\mathcal{C}^p$ and invertible. Finally, we introduce the following notation

$$H(q) = M^{-1}(q)G(q)W^{-1}(q), \tag{15}$$

which is also assumed to be of class $\mathcal{C}^p$.

Moreau's time–stepping scheme extended with a θ–method The numerical time integration of the MDI (13) is performed on an interval $(t_k, t_{k+1}]$ of length h as follows ($\theta \in [0,1]$):

$$\begin{cases} M(q_{k+\theta})(v_{k+1} - v_k) - hF(t_{k+\theta}, q_{k+\theta}, v_{k+\theta}) = p_{k+1} = G(q_{k+\theta})P_{k+1}, & \text{(16a)} \\ q_{k+1} = q_k + hv_{k+\theta}, & \text{(16b)} \\ U_{k+1} = G^T(q_{k+\theta})\, v_{k+1} & \text{(16c)} \\ -P_{k+1} \in N_{T_{\mathbb{R}^m_+}(\bar{g}_{k+\gamma})}(U_{k+1} + eU_k), & \text{(16d)} \\ \bar{g}_{k+\gamma} = g(q_k) + h\gamma U_k, \quad \gamma \in [0,1]. & \text{(16e)} \end{cases}$$

where the following approximations are considered

$$v_{k+1} \approx v^+(t_{k+1}); \quad U_{k+1} \approx U^+(t_{k+1}); \quad p_{k+1} \approx \mathrm{d}i(]t_k, t_{k+1}]), \quad P_{k+1} \approx \mathrm{d}I(]t_k, t_{k+1}]). \tag{17}$$

The value $\bar{g}_{k+\gamma}$ is a prediction of the constraint which allows the computation of the tangent cone $T_{\mathbb{R}^m_+}(\bar{g}_{k+1})$. The inclusion can be stated equivalently as a *conditional complementarity condition* for all $\alpha \in [1 \dots m] \in \mathcal{I}$,

$$\text{if} \quad \bar{g}^\alpha_{k+\gamma} \leqslant 0 \text{ then } 0 \leqslant U^\alpha_{k+1} + eU^\alpha_k \perp P^\alpha_{k+1} \geqslant 0, \text{otherwise } P^\alpha_{k+1} = 0. \tag{18}$$

The convergence of Moreau's time stepping scheme has been shown in [Monteiro Marques, 1993, Mabrouk, 1998, Stewart, 1998, Dzonou and Monteiro Marques, 2007] under various assumptions mainly with $\theta \in \{0, 1\}$. For the sake of readability, we will introduce the following short notation in the sequel $M_{k+\theta} = M(q_{k+\theta}), W_{k+\theta} = W(q_{k+\theta}), H_{k+\theta} = H(q_{k+\theta})$ and $F_{k+\theta} = F(t_{k+\theta}, q_{k+\theta}, v_{k+\theta})$.

Remark 3 *The projection of the velocity onto the tangent cone of $\mathbb{R}^n_+$ yield a slight violation of the constraints in generalized coordinates which occurs at the impact. The violation of the discrete coordinate can be corrected by adding another multiplier on the position level leading to the following scheme:*

$$\begin{cases} M_{k+\theta}(v_{k+1} - v_k) - hF_{k+\theta} = p_{k+1} = G_{k+\theta}P_{k+1}, & \text{(19a)} \\ q_{k+1} = q_k + hv_{k+\theta} + G(q_{k+\theta})\tau_{k+1}, & \text{(19b)} \\ U_{k+1} = G^T_{k+\theta}\, v_{k+1} & \text{(19c)} \\ -P_{k+1} \in N_{T_{\mathbb{R}^m_+}(\bar{g}_{k+1})}(U_{k+1} + eU_k), & \text{(19d)} \\ -\tau_{k+1} \in N_{\mathbb{R}^m_+}(g_{k+1}), & \text{(19e)} \\ \bar{g}_{k+1} = g(q_k) + h\gamma U_k, \quad \gamma \in [0, 1]. & \text{(19f)} \end{cases}$$

The multiplier τ_{k+1} has no physical meaning. It is an artificial projection embedded into the Moreau's time-stepping scheme to satisfy the constraints at the discrete times. It is very similar to the GGL algorithm proposed by [Gear et al., 1985] in solving the drift problem in DAE theory after an index reduction procedure. It is noteworthy that this scheme has no rigorous convergence proof and can exhibit some unstable behavior on large-scale examples with quite large time–steps.

2.1 Empirical order of convergence

Although the Moreau scheme enjoys some convergence results, no general result has been proved concerning its local order of consistency and global order of convergence. We propose to end this section with an empirical measure of the error of convergence on Examples 1 and 2.

Measuring errors In order to evaluate the order of accuracy on simple examples, we need to use a norm which is consistent with the BV functions and then to introduce a notion of convergence with provides us with a reasonable substitute to the uniform convergence for the uniformly continuous functions: the convergence in the sense of filled-in graph introduced by Moreau [Moreau, 1978]. Shortly, for a LBV function $f : [0, T] \mapsto \mathbb{R}^n$, we define the filled-in graph, $gr^\star(f)$ by adding line segments to the graph of f in such a way that all the gaps are filled:

$$\text{gr}^\star(f) = \{(t, x) \in [0, T] \times \mathbb{R}^n, 0 \leqslant t \leqslant T \text{ and } x \in [f(t^-), f(t^+)])\}. \tag{20}$$

Such graphs are closed bounded subsets of $[0, T] \times \mathbb{R}^n$, hence, we can use the Hausdorff distance $h^\star(\text{gr}^\star(f), \text{gr}^\star(g))$ between two such sets with a suitable metric $d((t, x), (s, y)) = \max\{|t - s|, \|x - y\|\}$. Thanks to this Hausdorff distance we are able to measure the error with respect to a reference solution given on our examples by an analytical result. When an analytical solution is known, an equivalent grid-function norm to the function norm in $\mathcal{L}_p(I, I\!R^n)$ defined by

$$\|e\|_p = \left(h \sum_{i=0}^{N} |f_i - f(t_i)|^p \right)^{1/p}, 1 \leqslant p < +\infty, \tag{21}$$

can be used. The computational effort for $\|e\|_p$ is lesser than the Hausdorff distance for piecewise continuous analytical function which is expensive. On the Figure 2, it is possible to check that the empirical order of Moreau's scheme is near to 1 in Hausdorff norm $h^\star(\cdot)$ and the $\|\cdot\|_1$ norm even if one of the example has an accumulation of impacts. In the uniform norm, the convergence can not be observed.

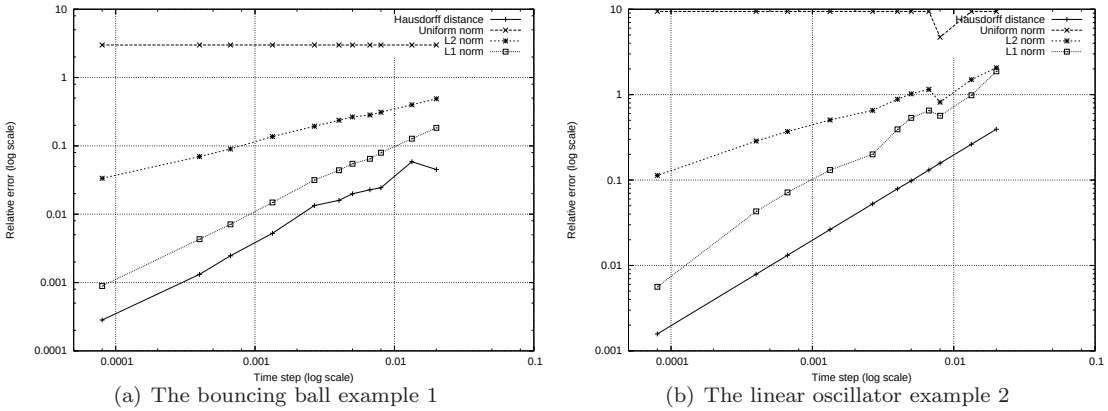

(a) The bouncing ball example 1 (b) The linear oscillator example 2

Figure 2: Empirical order of convergence of the Moreau's time-stepping scheme.

3 The Schatzman–Paoli's time–stepping scheme

The Schatzman–Paoli's scheme [Paoli and Schatzman, 1999] is given directly by a time–stepping scheme on the generalized coordinates q subjected to a projection onto the admissible set K. For a non trivial mass matrix, in the multi-contact case and with a θ-method, the following scheme can be viewed as an extension of the Schatzman–Paoli's scheme

$$\begin{cases} M(q_{k+1})(q_{k+1} - 2q_k + q_{k-1}) - h^2 \tilde{F}_{k+\theta} = p_{k+1}, & \text{(22a)} \\ v_{k+1} = \dfrac{q_{k+1} - q_{k-1}}{2h}, & \text{(22b)} \\ -p_{k+1} \in N_K \left(\dfrac{q_{k+1} + e q_{k-1}}{1+e} \right), & \text{(22c)} \end{cases}$$

where N_K defined the normal cone to the admissible set K. For an admissible set defined by a finite set of unilateral constraints,

$$K = \{q \in \mathbb{R}^n, y = g(q) \geqslant 0\}, \tag{23}$$

the inclusion into the normal can be recast under some constraints qualification conditions as a nonlinear complementarity problem of the form

$$\begin{cases} y_{k+1} = g\left(\dfrac{q_{k+1} + e q_{k-1}}{1+e} \right) \\ p_{k+1} = G\left(\dfrac{q_{k+1} + e q_{k-1}}{1+e} \right) P_{k+1} \\ 0 \leqslant y_{k+1} \perp \mu_{k+1} \geqslant 0 \end{cases} \tag{24}$$

The convergence of Schatzman-Paoli's time stepping schemes has been shown in [Paoli and Schatzman, 2002a,b, Paoli, 2005] under various assumptions.

3.1 Qualitative comparison with Moreau's scheme

For the sake of simplicity, let us consider a nonsmooth multi–body system subjected to simple linear constraints $q \geqslant 0$. Providing that M is symmetric positive definite in order to define an associated metric and using some basics in Convex Analysis, we can write [Brogliato, 1999]:

$$\begin{array}{rcl} M(x-y)-b & \in & -\lambda N_K(x), \lambda > 0 \\ & \Updownarrow & \\ x & = & \mathrm{argmin}_{z\in K} \dfrac{1}{2}(z-y)^T M(z-y) - (z-y)^T b \\ & \Updownarrow & \\ x & = & \mathrm{prox}_M\left(K; y + M^{-1}b\right) \end{array} \tag{25}$$

Moreau's time–stepping scheme can be written in terms of the proximal operator as

$$v_{k+1} + ev_k = \mathrm{prox}_{M(q_{k+1})}\left(T_{\mathbb{R}^n_+}(\tilde{q}_{k+1}); (1+e)v_k + hM^{-1}(q_k+1)F(t_{k+\theta}, q_{k+\theta}, v_{k+\theta})\right) \tag{26}$$

and Schatzman–Paoli's scheme as

$$q_{k+1} + eq_{k-1} = \mathrm{prox}_{M(q_{k+1})}\left(\mathbb{R}^n_+; 2q_k - (1-e)q_{k-1} + h^2M^{-1}(q_k+1)F(t_{k+\theta}, q_{k+\theta}, v_{k+\theta})\right) \tag{27}$$

On the qualitative point of view, the main difference between these two schemes if the physical nature of the projected variable. In the Moreau's scheme, the variable which is projected is homogeneous to a velocity. One of the interesting remark is that the Newton's impact law is respected for the discrete velocity in a very natural way. This fact leads to a straightforward interpretation of the discrete multiplier as an impulse. However, the projection of the velocity onto the tangent cone of $\mathbb{R}^n_+$ yield a slight violation of the constraints in generalized coordinates which occurs at the impact.

In the Schatzman–Paoli scheme, the generalized coordinates is directly projected onto an admissible set. The result is that there no violation of the discrete constraints. On the contrary, the discrete velocity do not satisfy the Newton's impact law and the multiplier involves in the projection of the coordinates has no direct physical meaning. The Newton impact law is only respected after several steps. On the other hand, on the simple linear oscillator example, the scheme does not generate artificial rebound in presence of flexibility.

3.2 Empirical Order

We can see on the Figure 3 that the order of convergence of the time-stepping scheme is one in Hausdorff distance and $\|\cdot\|_1$ grid norm. In uniform norm, any convergence can be observed.

4 Local Order Estimates for Moreau's Time–Stepping Scheme

The goal of this section is to evaluate the local truncation error for Moreau's scheme as

$$e = \left[\begin{array}{c} e_v \\ e_q \end{array}\right] = \left[\begin{array}{c} v^+(t_k+h) - v_{k+1} \\ q(t_k+h) - q_{k+1} \end{array}\right], \tag{28}$$

starting with the exact solution as initial data, *i.e.*, $q_k = q(t_k)$ and $v_k = v^+(t_k)$. Under Assumption 1, the error can be estimated by

$$e_q = \int_{t_k}^{t_{k+1}} v(s)\,ds - h(\theta v_{k+1} + (1-\theta)v_k), \tag{29}$$

and

$$e_v = \int_{(t_k, t_{k+1}]} \mathrm{d}v - hM^{-1}_{k+\theta}F_{k+\theta} - M^{-1}_{k+\theta}p_{k+1}. \tag{30}$$

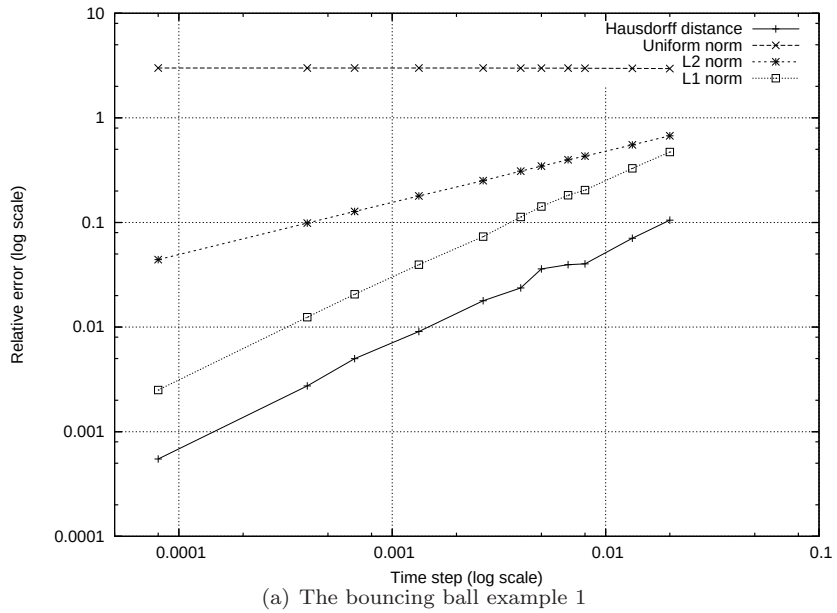

(a) The bouncing ball example 1

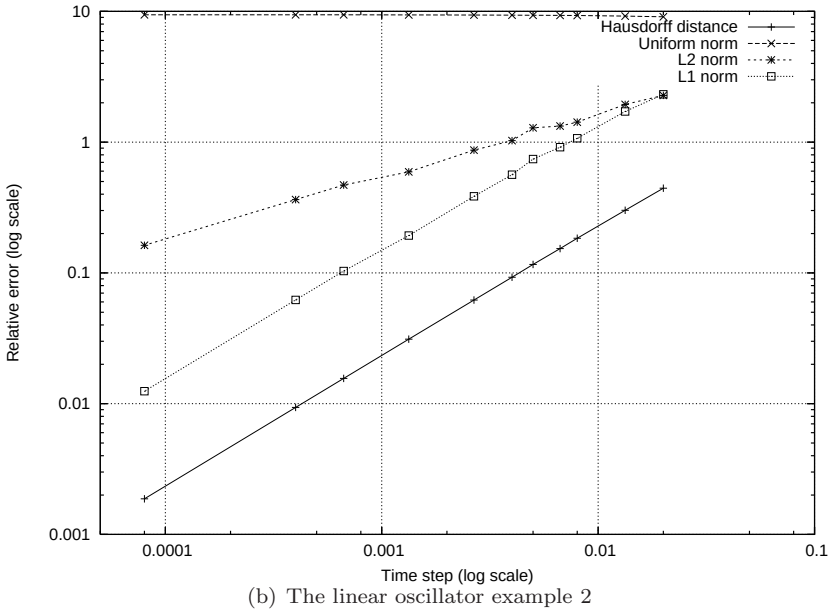

(b) The linear oscillator example 2

Figure 3: Empirical order of convergence of the Schatzman-Paoli's time-stepping scheme.

Example 3 (Bouncing Ball continued) *Let us consider the bouncing ball example (Example 1) and a time interval such that the impacting time t_* belongs to $(t_k, t_{k+1}]$. The error is*

$$\begin{cases} e_v = -(1+e)[v_k + hf\sigma] \\ e_q = -q_k - h(e(1-\sigma+1))v_k - fh^2[e(1-\sigma)\sigma + \frac{1}{2}(1-\sigma)^2 + \theta] \end{cases} \quad \text{if} \quad p_{k+1} = 0$$
$$\begin{cases} e_v = -hf[1-\sigma-e\sigma] \\ e_q = -q_k - h((1+e)(1-\theta) - e\sigma)v_k - fh^2(e(1-\sigma)\sigma + \frac{1}{2}(1-\sigma)^2) \end{cases} \quad \text{if} \quad p_{k+1} > 0, \tag{31}$$

The approximate solution of the Moreau scheme depends on the forecast of the active constraints, i.e. $\bar{g}_{k+1} = q_k + \gamma h v_k$. Using the fact that $q(t_*) = q_k + v_k\sigma h + \frac{1}{2}(\sigma h)^2 = 0$, we obtain that $q_k = -\sigma v_k h - \frac{1}{2}f(\sigma h)^2$ and

$$\begin{cases} e_v = -(1+e)[v_k + hf\sigma] \\ e_q = -h(e(1-\sigma+1)-\sigma)v_k - fh^2[e(1-\sigma)\sigma + \frac{1}{2}(1-\sigma)^2 - \frac{1}{2}(\sigma)^2 + \theta] \end{cases} \quad \text{if} \quad p_{k+1} = 0,$$
$$\begin{cases} e_v = -hf[1-\sigma-e\sigma] \\ e_q = -h((1+e)(1-\theta-\sigma))v_k - fh^2(e(1-\sigma)\sigma + \frac{1}{2}(1-\sigma)^2 - \frac{1}{2}(\sigma)^2) \end{cases} \quad \text{if} \quad p_{k+1} > 0, \tag{32}$$

Near the finite accumulation of impact at time $t = 3$, we can also try to evaluate the error. Let us consider a time step such that $[t_k, t_{k+1}] = [3-h, 3+h]$ and n_0 such that $h \in [1/2^{n_0}, 1/2^{n_0-1}]$. The local error in velocity is given if the impact is detected $p_{k+1} > 0$ by

$$e_v = v(3+h) - v_{k+1} = -2h - \frac{3}{2^{n_0}}. \tag{33}$$

As $h \to 0$, we have $n_0 \to 0$, and $\dfrac{1}{2^{n_0}} = \mathcal{O}(h)$ and then $e_v = \mathcal{O}(h)$.

For Example 3, the consistency error in generalized coordinates e_q is always in $\mathcal{O}(h)$ and it is difficult to obtain a better approximation except for very particular choices of e and σ which can not be chosen a priori by the user. The consistency error in velocity e_v is $\mathcal{O}(1)$ if the impact is not correctly forecast. In this case, there is no chance to reduce the amplitude of the consistency error with the time–step. The situation may happen if the activation of the constraint based on the prediction $\bar{g}_{k+1}$ is not correct, which systematically occurs in this examples with $\gamma = 0$.

4.1 General estimates for the local error

Lemma 1 *Let $I = [t_k, t_{k+1}]$. Let us assume that the function $f \in BV(I, I\!R^n)$. Then we have the following inequality for the θ–method, $\theta \in [0,1]$,*

$$\left\| \int_{t_k}^{t_{k+1}} f(s)\,ds - h(\theta f(t_{k+1}) + (1-\theta)f(t_k)) \right\| \leqslant C(\theta)(t_{k+1}-t_k)\, var(f, I), \tag{34}$$

where $var(f, I) \in I\!R$ is the variation of f on I and $C(\theta) = \theta$ if $\theta \geqslant 1/2$ and $C(\theta) = 1-\theta$ otherwise. Furthermore, the value of $C(\theta)$ yields a sharp bound in (34).

proof Let us consider the function $\varphi_\theta : [t_k, t_{k+1}] \to I\!R$ such that

$$\varphi_\theta(t) = (2\theta - 1)(t - t_{k+1}) + h\theta \text{ for } \theta \in [0,1] \text{ with } h = t_{k+1} - t_k. \tag{35}$$

Using the integration by parts for the differential measure $\mathrm{d}f$ associated with f (see [Moreau, 1988b]), we get

$$\int_{[t_k, t_{k+1}]} \varphi_\theta(t)\mathrm{d}f = h(\theta f(t_{k+1}) + (1-\theta)f(t_k)) - \int_{t_k}^{t_{k+1}} f(s)\,ds. \tag{36}$$

The integral term involving the differential measure $\mathrm{d}f$ can be bounded as follows (see [Moreau, 1988b])

$$\left\| \int_{[t_k,t_{k+1}]} \varphi_\theta(t) \mathrm{d}f \right\| \leqslant \max_{t\in[t_k,t_{k+1}]} |\varphi_\theta(t)| \operatorname{var}(f, I) \tag{37}$$

since $\varphi_\theta(\cdot)$ is uniformly continuous on $[t_k, t_{k+1}]$ and $f \in BV(I, I\!R^n)$. Computing the value of the maximum value $C(\theta)$ gives,

$$\max_{t\in[t_k,t_{k+1}]} |\varphi_\theta(t)| = \max_{t\in[t_k,t_{k+1}]} |(2\theta-1)(t-t_{k+1}) + h\theta| = \begin{cases} h\theta, \text{ if } \theta \geqslant \dfrac{1}{2} \\ h(1-\theta), \text{ if } \theta \leqslant \dfrac{1}{2} \end{cases} \triangleq C(\theta)h \tag{38}$$

The result (34) is obtained from (36) and (37). In order to prove that the bound is sharp, let us consider for instance that f is given by $f(t) = -t$ for $t \in (t_k, t_{k+1})$, $f(t_k) = -1$, and $f(t_{k+1}) = \beta$. Choosing $\beta = -1 + \theta/2$ for $0 \leqslant \theta < 1/2$ and $\beta = (1-5\theta)/(4\theta)$ for $1/2 \leqslant \theta \leqslant 1$, a straightforward calculus shows that the bound is attained.

Proposition 1 *Let $I = [t_k, t_{k+1}]$. Under Assumptions 1 and 2, the local order of consistency of the Moreau time–stepping scheme for the generalized coordinates is $e_q = \mathcal{O}(h)$ and at least for the velocities $e_v = \mathcal{O}(1)$.*

proof The estimate e_v on the velocity is trivial if we recall that $M_{k+\theta}^{-1}(F_{k+\theta} - p_{k+1}$ is bounded on $[t_k, t_{k+1}]$. The B.V. function $v(\cdot)$ is also bounded on $[t_k, t_{k+1}]$ then we have that e_v is also bounded. Therefore, we obtain $e_v = \mathcal{O}(1)$. Using Lemma 1 for $v^+ \in BV(I, I\!R^n)$, we get

$$\left\| \int_{t_k}^{t_{k+1}} v(s)\, ds - h(\theta v^+(t_{k+1}) + (1-\theta)v^+(t_k)) \right\| \leqslant C(\theta)h \operatorname{var}(v^+, I), \tag{39}$$

Since $v_k = v^+(t_k)$ and $v_{k+1} = v(t_{k+1}) + \mathcal{O}(1)$, we obtain for (39)

$$\left\| \int_{t_k}^{t_{k+1}} v(s)\, ds - h(\theta v_{k+1} + (1-\theta)v_k) - \theta\mathcal{O}(h)) \right\| = \|e_q - \theta\mathcal{O}(h)\| \leqslant C(\theta)h \operatorname{var}(v^+, I), \tag{40}$$

which completes the proof. □

4.2 Definition of Index sets

In order to improve the estimate on velocity in Proposition 1, we need to introduce several index sets of constraints given by the following definition.

Definition 2 (Index sets $\mathcal{I}_*$, $\mathcal{I}(t)$ and $\mathcal{I}_k$) *Three specific index sets of constraints are defined :*

1. *the index set $\mathcal{I}_*$ of unilateral constraints such that the exact solution has an impact at t_**

$$\mathcal{I}_* = \{\alpha \in \mathcal{I} \mid g^\alpha(q) = 0, P^\alpha \geqslant 0, U^{\alpha,+}(t_*) - U^{\alpha,-}(t_*) = -(1+e)U^{\alpha,-}(t_*) > 0\} \subset \mathcal{I}, \tag{41}$$

2. *the index set $\mathcal{I}(t)$ of unilateral constraints such that the exact solution has a persistent contact*

$$\mathcal{I}(t) = \{\alpha \in \mathcal{I} \mid g^\alpha(q) = 0, \lambda^\alpha(t) \geqslant 0, U^{\alpha,+}(t) = U^{\alpha,-}(t) = 0\} \subset \mathcal{I}, \tag{42}$$

3. *the index set $\mathcal{I}_k$ is of unilateral constraints such that the approximate solution with the exact initial data $q(t_k), v(t_k)$ encounters an impact in the time–step $(t_k, t_{k+1}]$*

$$\mathcal{I}_k = \{\alpha \in \mathcal{I} \mid \bar{g}_{k+1}^\alpha \leqslant 0, P_{k+1}^\alpha \geqslant 0, U_{k+1}^\alpha - U_k^\alpha = -(1+e)U_k^\alpha\} \subset \mathcal{I}. \tag{43}$$

4.3 Smooth motion with persistent contacts

Assumption 3 *Let us assume that the system evolves in a smooth phase with only persistent contacts in* $(t_k, t_{k+1}]$*. In particular, we assume a constant index set* $\mathcal{I}(t)$ *for all* $t \in (t_k, t_{k+1}]$ *and*

$$\mathrm{d}I^\alpha = \lambda^\alpha(t)\mathrm{d}t, \alpha \in \mathcal{I}(t) \text{ or equivalently } \mathrm{d}i = r(t)\mathrm{d}t. \tag{44}$$

Proposition 2 *Let us assume that Assumptions 2 and 3 hold. If* $\mathcal{I}(t) = \mathcal{I}_k$ *for all* $t \in (t_k, t_{k+1}]$ *and* $U_k^\alpha = 0$ *for all* $\alpha \in \mathcal{I}_k$ *, then the local order of consistency of the scheme is* $e_v = \mathcal{O}(h^2)$ *and* $e_q = \mathcal{O}(h^2)$*.*

proof In the case that $\mathcal{I}(t) = \mathcal{I}_k$ for all $t \in (t_k, t_{k+1}]$, the Moreau time–stepping amounts to solve

$$\begin{cases} M_{k+\theta}(v_{k+1} - v_k) - hF_{k+\theta} = G_{k+\theta}P_{k+1}, \\ q_{k+1} = q_k + hv_{k+\theta}, \\ U_{k+1} = G_{k+\theta}^T v_{k+1} = 0. \end{cases} \tag{45}$$

Thanks to Assumption 2, an unique solution of class $\mathcal{C}^{p+1}$ is expected with a multiplier of class $\mathcal{C}^p$. The time–stepping scheme can be therefore be studied as an application of the backward Euler Scheme or a θ–method for an index-2 DAE. The results on the local order of convergence obtained for implicit Runge–Kutta method [Hairer et al., 1987, Hairer and Wanner, 1996] or for backward differentiation formulas [Lötstedt and Petzold, 1986, Brenan et al., 1989] can be straightforwardly extended to obtain the proof of the lemma. □

4.4 Continuous Lagrange multiplier with a single impact in the time–step

In this section, the following assumptions are stated

Assumption 4 *Let us assume that only a single impact at* $t_* \in (t_k, t_{k+1}]$ *occurs in the time interval. Neglecting the singular continuous part of the decomposition of* $\mathrm{d}i$ *and* $\mathrm{d}v$*, the following decomposition is assumed*

$$\mathrm{d}i = p\delta_{t_*} + r(t)\mathrm{d}t, \quad \text{and} \quad \mathrm{d}v = (v^+(t_*) - v^-(t_*))\delta_{t_*} + u'(t)\mathrm{d}t, \tag{46}$$

where the multiplier $r(\cdot)$ *and the velocity* $u(\cdot)$ *are assumed to be absolutely continuous on* $[t_k, t_{k+1}]$*.*

Proposition 3 *Let us assume that Assumptions 1, 2 and 4 hold.*

1. *If* $\mathcal{I}_* = \mathcal{I}_k$*, then the local order of consistency of the Moreau time stepping scheme for the velocity is* $e_v = \mathcal{O}(h)$*.*
2. *If* $\mathcal{I}_* \neq \mathcal{I}_k$*, then we retrieve the rough estimate of Proposition 1, that is* $e_v = \mathcal{O}(1)$*.*

proof Under Assumption 4, the MDI (14) can be decomposed to obtain

$$M(q(t))u'(t) = F(t, q(t), v^+(t)) + r(t), \quad \mathrm{d}t\text{–almost everywhere} \tag{47}$$

and

$$M(q(t_*))^{-1}(v^+(t_*) - v^-(t_*) = p, \quad \text{for } t = t_*, \tag{48}$$

where the differential measure $\mathrm{d}v$ has been decomposed as

$$\mathrm{d}v = u'(t)\,\mathrm{d}t + (v^+(t_*) - v^-(t_*))\delta_{t_*} = M(q(t))^{-1}[F(t, q(t), v^+(t)) + r(t)]\,\mathrm{d}t + M(q(t_*))^{-1}p\delta_{t_*} \tag{49}$$

The function $u'(\cdot)$ is equal to $v'(\cdot)$ dt-almost everywhere. In this case, the error e_v is

$$\begin{aligned} e_v &= \int_{t_k}^{t_{k+1}} M^{-1}(q(t))[F(t,q(t),v^+(t))+r(t)]\,\mathrm{d}t \\ &\quad -hM_{k+\theta}^{-1}F_{k+\theta}+M(q(t_*))^{-1}p-M_{k+\theta}^{-1}p_{k+1}. \end{aligned} \tag{50}$$

Since the function $t\mapsto M(q(t))^{-1}r(t)$ is assumed to be continuous, it is bounded on $[t_k,t_{k+1}]$. The mapping f and M are assumed to be of class $C^p, p\geqslant 1$ and $v^+\in BV([t_k,t_{k+1}],I\!R^n)$, therefore the function $t\mapsto M^{-1}(q(t))f(t,q(t),v^+(t))$ is also bounded on $[t_k,t_{k+1}]$. The following estimate for the integral term of (50) is then deduced

$$\int_{t_k}^{t_{k+1}} M^{-1}(q(t))[F(t,q,v^+)+r(t)]\,\mathrm{d}t - hM_{k+\theta}^{-1}F_{k+\theta}=\mathcal{O}(h). \tag{51}$$

The remaining term in (50) can be computed as

$$\begin{aligned} M(q(t_*))^{-1}p-M_{k+\theta}^{-1}p_{k+1} &= M(q(t_*))^{-1}G(q(t_*))W^{-1}(q(t_*))[U^+(t_*)-U^-(t_*)] \\ &\quad -M_{k+\theta}^{-1}G_{k+\theta}W_{k+\theta}^{-1}[U_{k+1}-U_k-hG_{k+\theta}^TM_{k+\theta}^{-1}F_{k+\theta}], \end{aligned} \tag{52}$$

and introducing the notation (15), we have

$$\begin{aligned} M(q(t_*))^{-1}p-M_{k+\theta}^{-1}p_{k+1} &= H(q(t_*))[U^+(t_*)-U^-(t_*)] \\ &\quad -H_{k+\theta}[U_{k+1}-U_k-hG_{k+\theta}^TM_{k+\theta}^{-1}F_{k+\theta}]. \end{aligned} \tag{53}$$

The mapping $H(q)$ is assumed to be of class $\mathcal{C}^p, p\geqslant 1$ therefore

$$H(q_{k+\theta})-H(q)=\nabla_q^TH(q)(q_{k+\theta}-q)+\mathcal{O}(\|q_{k+\theta}-q\|^2). \tag{54}$$

where the gradient of the matrix $H(q)$ which is a 3–order tensor is denoted by $\nabla_q^TH(q)$. Let us now evaluate $q_{k+\theta}-q(t_*)=(1-\theta)q(t_k)+\theta q_{k+1}-q(t_*)$. By Proposition 1, we have $q_{k+1}=q(t_{k+1})+\mathcal{O}(h)$. Since v is bounded, we have also $q(t_{k+1})=q(t_k)+\mathcal{O}(h)$ and then $q_{k+1}=q(t_k)+\mathcal{O}(h)$. We can write $q_{k+\theta}-q(t*)=q(t_k)-q(t^*)+\mathcal{O}(h)$. The boundedness of v gives

$$q_{k+\theta}-q(t*) = \mathcal{O}(h). \tag{55}$$

Using (54) and (55) and the regularity assumption on H, we obtain

$$H(q_{k+\theta})-H(q(t_*))=\mathcal{O}(h). \tag{56}$$

For the expression (53), we get

$$M(q(t_*))^{-1}p-M_{k+\theta}^{-1}p_{k+1}=H_{k+\theta}[U^+(t_*)-U^-(t_*)-[U_{k+1}-U_k-hG_{k+\theta}^TM_{k+\theta}^{-1}F_{k+\theta}]]+\mathcal{O}(h). \tag{57}$$

Let us define in (57) the error e_U in terms of local velocity at contact as,

$$e_U=\left[U^+(t_*)-U^-(t_*)-[U_{k+1}-U_k-hG_{k+\theta}^TM_{k+\theta}^{-1}F_{k+\theta}]\right]. \tag{58}$$

Depending on the constraint $\alpha\in\mathcal{I}$ belongs or not to the index sets $\mathcal{I}_*$ and $\mathcal{I}_k$, the error e_U can be estimated as follows.

Case 1 Let us assume that $\mathcal{I}_*=\mathcal{I}_k$.

For all $\alpha\in\mathcal{I}_*\cap\mathcal{I}_k$, we have $U^{+,\alpha}(t_*)=-eU^{-,\alpha}(t_*)$ and $U_{k+1}^\alpha=-eU_k^\alpha$. The error term e_U^α is written

$$\begin{aligned} e_U^\alpha &= -(1+e^\alpha)(U^{-,\alpha}(t_*)-U_k^\alpha)+hG_{k+\theta}^{T,\alpha}M_{k+\theta}^{-1}F_{k+\theta} \\ &= -(1+e^\alpha)\int_{t_k}^{t_*}U'^\alpha(t)\,\mathrm{d}t+hG_{k+\theta}^{T,\alpha}M_{k+\theta}^{-1}F_{k+\theta} \end{aligned} \tag{59}$$

Since $U'^{\alpha}(t) = G^T(q(t))M^{-1}(q(t))\left[F(t,q(t),v^+(t)) + r(t)\right]\,\mathrm{d}t$ almost everywhere, we have

$$\int_{t_k}^{t_*} U'^{\alpha}(t)\,\mathrm{d}t = \int_{t_k}^{t_*} G^T(q(t))M^{-1}(q(t))\left[F(t,q(t),v^+(t)) + r(t)\right]\,\mathrm{d}t. \tag{60}$$

With the same argument of boundedness of $G^T(q(t))M^{-1}(q(t))\left[F(t,q(t),v^+(t)) + \lambda(t)\right]$, we get

$$\int_{t_k}^{t_*} U'^{\alpha}(t)\,\mathrm{d}t = \mathcal{O}(h), \tag{61}$$

and therefore $e_U = \mathcal{O}(h)$. By Definition 2, we have $P^{\beta} = P^{\beta}_{k+1} = 0$ for all $\beta \notin \mathcal{I}_* \cap \mathcal{I}_k$. We conclude that $e^{\beta}_U = 0$. From (51), (57) and (61), the consistency error is $e_v = \mathcal{O}(h)$.

Case 2 Let us assume that $\mathcal{I}_* \neq \mathcal{I}_k$. For all $\alpha \notin \mathcal{I}_*$ and $\alpha \in \mathcal{I}_k$, the error term e^{α}_U is

$$\begin{array}{rcl} e^{\alpha}_U & = & -(1+e^{\alpha})(U^{\alpha}_k) + hG^{T,\alpha}_{k+\theta}\Phi_{v,k} = \mathcal{O}(1) \quad \text{for all } \alpha \notin \mathcal{I}_* \text{ and } \alpha \in \mathcal{I}_k, \\ e^{\alpha}_U & = & -(1+e)(U^-(t_*)) = \mathcal{O}(1) \text{ for all } \alpha \in \mathcal{I}_* \text{ and } \alpha \notin \mathcal{I}_k. \end{array} \tag{62}$$

From (51), (53), and (62), the consistency error for velocities is $e_v = \mathcal{O}(1)$. □

4.5 Comments on the local error estimates of Proposition 1 and 3

The local error estimates obtained in this section are quite rough. In summary, the following points can be outlined

- The local error in coordinates is $e_q = \mathcal{O}(h)$ and it can not be improved as the the bouncing ball example shows. Note that even is the velocity is exactly integrated in time, we can not expect a better order for the numerical integration of q as Lemma 1 shows.
- The local error in velocity is at least $e_v = \mathcal{O}(1)$ is the impact is not forecast. In practice, this situation is usual. For instance, if $\gamma = 0$ is chosen in (16e), the impact is not forecast in the correct time–interval for the academic examples presented in this paper. It illustrates the possible convergence problem that we can have in uniform norm as we mentioned in Section 2.1.
- The local error in velocity is at least $e_v = \mathcal{O}(h)$ with only one impact in the time-interval and a well-forecast impact. If there is no right accumulation of impacts at any points, this result proof is sufficient in theory. Indeed, we can always find a sufficiently small time–step such that there is only one impact inside $(t_k, t_{k+1}]$. However, in the numerical practice this result is not satisfactory because such a time step will vanish at the accumulation of impacts. An open issue is to prove that we have $e_v = \mathcal{O}(h)$ in a time–step which contains a well–forecast finite accumulation as we made at the end of Section 3 for Example 1.

5 An attempt at adjusting the time–step size for Moreau's scheme

5.1 Practical local error estimates in standard smooth case ans automatic step–size control

In order to control the time step, an practical estimation of the consistency error is needed. Let us consider the standard case of ODE given by $\dot{x} = f(x,t)$. A standard error estimation for a scheme with a local order in $\mathcal{O}(h^{p+1})$ may be based on a extrapolation with halved time–steps (see [Hairer et al., 1993, pages 164–172]) and yields a practical error estimate such that:

$$e_2 = x(t_0+h) - x_2 = \frac{x_{1/2} - x_1}{2^p - 1} + \mathcal{O}(h^{p+2}). \tag{63}$$

where $x_1, x_{1/2}$ and x_2 are the values obtained by the numerical time–integration with halved time–steps.

5.2 Automatic step size control

Based on a chosen local error estimate, the time–step selection method can be designed following the standard procedure exposed in [Hairer et al., 1993]. For a given absolute tolerance vector $atol \in \mathbb{R}^n$ and a relative tolerance vector $rtol \in \mathbb{R}^n$, The optimal step size is chosen as

$$h_{\text{opt}} = h \left(\frac{1}{\text{error}} \right)^{1/(p+1)} \tag{64}$$

with

$$\text{error} = \left\| \left[\frac{e_k}{atol + rtol \max(x_{0,k}, x_k)}, k \in 1 \dots n \right] \right\| \tag{65}$$

Usually, the step size is not allowed to decrease or increase too fast, thanks to the following heuristic rule

$$h_{\text{new}} = h \min \left(\alpha_{max}, \max \left(\alpha_{min}, \alpha \left(\frac{1}{\text{error}} \right)^{1/(p+1)} \right) \right) \tag{66}$$

where α, α_{min} and α_{max} are some user parameters.

5.3 What can be done in nonsmooth situation ?

It seems obvious that an implementation which rely on the local error in velocity e_v is not a good idea since $e_v = \mathcal{O}(1)$ in practical situations. Indeed there is no chance that the error in $v(\cdot)$ will reduce with the time-step h.

Let us consider the estimate on the coordinates $e_q = \mathcal{O}(h)$. In this case, the error e_q will be proportional to h for sufficiently small h. Unfortunately, for such a estimate we can not apply standard error based on a extrapolation with halved time–steps mainly because $p = 0$ which reflects that fact that the error is not smoothly transported. The proposed approach is a heuristic which is only justify on the several examples presented in this paper. Clearly, a more thorough study is needed to confirm the good behavior of the approach on more complex systems. We propose to evaluate the error by

$$e_{q,1/2} \approx (q_{1/2} - q_1) \tag{67}$$

This practical estimation of the error recalls the oldest device of Runge cited by[Hairer et al., 1993, page 164]). For Example 1(the bouncing ball) and 2 (the linear oscillator), the results are depicted on Figure 4 where the CPU effort is plotted with respect to the global error $\|e\|_1$. The CPU effort is compared to the error with respect to the analytical solution. The CPU effort is counted as the number of numerical evaluations of the multiplier. The parameters of the automatic step size control are $\alpha_{\min} = 0.5$, $\alpha_{\max} = 5$ and $\alpha = 1.0$ and the simulation is performed for $T = 5$.

The preliminary conclusion is that we are able to reach reasonable accuracy without a huge CPU effort. The heuristic on this very simple works pretty well. However, this preliminary result has to be confirmed by a more thorough study on more complex examples.

5.4 A variable order approach

Another attempt has been made based on the inspection of the possible events in the time–interval. If an event is present, the local order of accuracy of the scheme is given by the Proposition 1. If there is no event in the time–interval, the local order of accuracy of the scheme is chosen as the same as the backward Euler scheme for index-2 DAE.

The last strategy amounts to guess first the order of consistency of the scheme on the current time–step, and then to evaluate an local error. Once, the step–size selection procedure is standard.

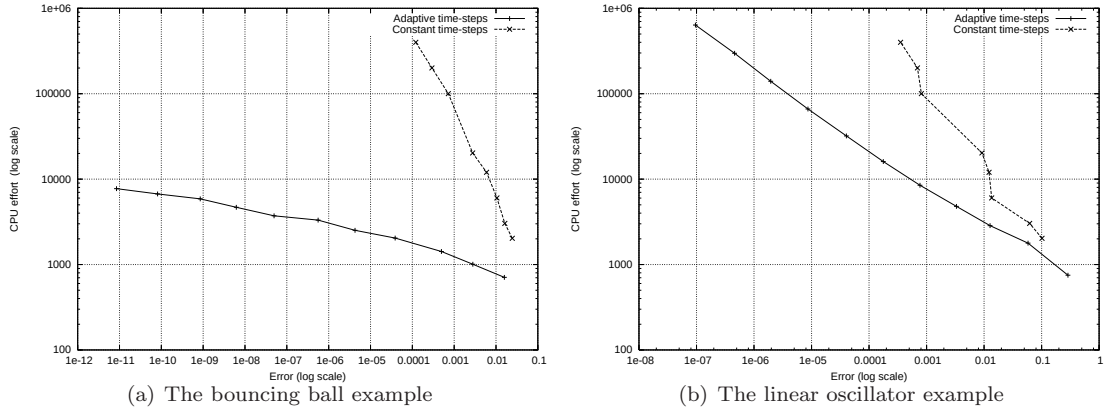

(a) The bouncing ball example (b) The linear oscillator example

Figure 4: Precision Work diagram for the Moreau's time-stepping scheme with the heuristic (67).

The goal of this approach is to save computational time when the motion is assumed to be smooth enough.

The local order of consistency is guessed by inspecting the so-called status of constraints. The status of the constraints is a vector, $s_k \in \mathbb{N}^m$ that is a discrete state. For each constraints $\alpha = 1 \dots m$, a integer value is assigned to the status $s_{k+1}(\alpha)$ such that

$$\begin{array}{ll} s_k(\alpha) = 0 & \text{if} \quad g_\alpha(q_k) > 0 \\ s_k(\alpha) = 1 & \text{if} \quad g_\alpha(q_k) \leqslant 0 \end{array} \tag{68}$$

Following the analysis of the Section 4, the order of the integration scheme is guessed by means of the following algorithm :

$$\begin{array}{lllllll} \text{If} & s_{k+1}(\alpha) = 0 & \text{and} & s_k(\alpha) = 0 & \text{then} & order_k(\alpha) = 1 & \text{(Free motion)} \\ \text{If} & s_{k+1}(\alpha) = 1 & \text{and} & s_k(\alpha) = 0 & \text{then} & order_k(\alpha) = 0 & \text{(impacting)} \\ \text{If} & s_{k+1}(\alpha) = 0 & \text{and} & s_k(\alpha) = 1 & \text{then} & order_k(\alpha) = 1 & \text{(losing contact)} \\ \text{If} & s_{k+1}(\alpha) = 1 & \text{and} & s_k(\alpha) = 1 & \text{then} & order_k(\alpha) = 1 & \text{(pertaining contact)} \end{array} \tag{69}$$

and

$$order_k = \min_{\alpha \in \mathcal{I}} \{order_k(\alpha)\} \tag{70}$$

Once the order is guessed, we apply the heuristic procedure (67) if $order_k = 0$ and the standard evaluation (63) otherwise.

The result are depicted on Figure 5. The gain is larger for the linear oscillator example mainly due to the fact that the smooth dynamics given by F is a little bit less simple than the constant dynamics of the bouncing ball example. The approach could lead to interesting results on problems with nonlinear smooth dynamics even if an adaptive time–step strategy is not very efficient on low-order time–stepping schemes. This remark is one of the main motivations for the development of higher–order schemes that we will presented in the next section.

6 Higher Order event–capturing time–stepping scheme

In this section, we propose a method to design a higher order time–stepping scheme which extends an original idea of Mannshardt [Mannshardt, 1978] for ordinary differential equations with discontinuities. The key idea of such schemes is based on a rough localization of the impact or events such as activations or deactivations of constraints into a so-called *critical time–step*. Choosing a method of order p with a time step h for integrating the smooth dynamics, the event is integrated over the critical time–step with a method of order q on the critical time–step. The length of the critical time–step denoted by $\bar{h}$ is driven such that $\bar{h}^{q+1} = \mathcal{O}(h^{p+1})$.

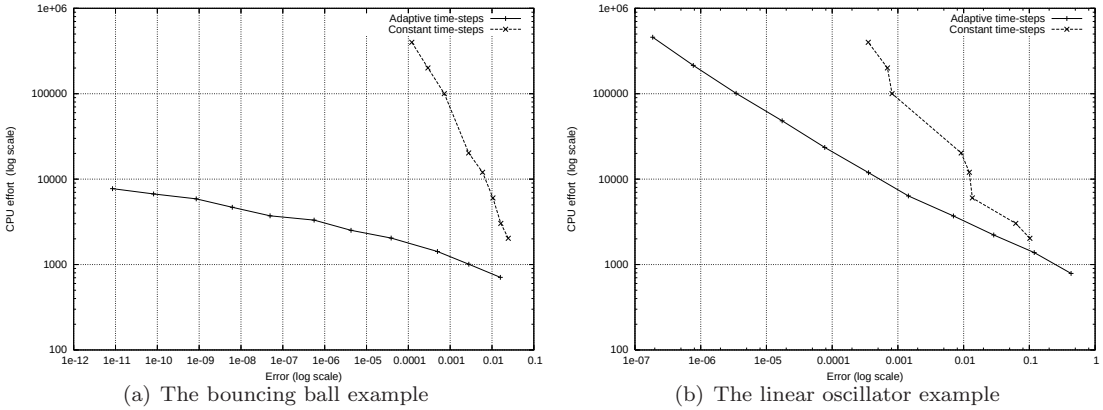

(a) The bouncing ball example (b) The linear oscillator example

Figure 5: Precision Work diagram for the Moreau's time-stepping scheme with variable order approach.

6.1 Integration of the smooth dynamics

Mainly for the sake of simplicity, the numerical integration on a smooth phase is made with a Runge–Kutta (RK) method on the following index-1 DAE,

$$\begin{cases} M(q(t))\dot{v}(t) = F(t, q(t), v(t)) + G(q)\lambda(t), \\ \dot{q}(t) = v(t), \\ \gamma(t) = G(q(t))\dot{v}(t) = 0. \end{cases} \tag{71}$$

In practice, the time–integration is performed for the following system

$$\begin{cases} M(q(t))\dot{v}(t) = F(t, q(t), v(t)) + G(q)\lambda(t), \\ \dot{q}(t) = v(t), \\ 0 \leqslant \gamma(t) = G(q(t))\dot{v}(t) \perp \lambda(t) \geqslant 0. \end{cases} \tag{72}$$

on time–interval I where the index set $\mathcal{I}(t)$ of active constraints is assumed to be constant on I and $\lambda(t) > 0$ for all $t \in I$. Using (72) rather than (71) allows one to detect events if the acceleration γ becomes nonnegative and/or if the multiplier λ vanishes. Using the standard notation for the RK methods (see [Hairer et al., 1993] for details), the complementarity problem that we have to solve at each time–step reads as

$$\begin{cases} t_{ki} = t_k + c_i h, \\ v_{k+1} = v_k + h \sum_{i=1}^{s} b_i V'_{ki}, \\ q_{k+1} = q_k + h \sum_{i=1}^{s} b_i V_{ki}, \\ V'_{ki} = M^{-1}(Q_{ki}) \left[F(t_{ki}, Q_{ki}, V_{ki}) + G(Q_{ki})\lambda_{ki} \right], \\ V_{ki} = v_k + h \sum_{j=1}^{s} a_{ij} V'_{nj}, \\ Q_{ki} = q_k + h \sum_{j=1}^{s} a_{ij} V_{nj}, \\ 0 \leqslant \gamma_{ki} = G(Q_{ki})V'_{ki} \perp \lambda_{ki} \geqslant 0. \end{cases} \tag{73}$$

Assumption 5 *Let I a smooth phase time–interval (see Definition 1). We assume that*

1. *the local order of the RK method (73) is p that is*

$$e_q = e_v = \mathcal{O}(h^{p+1}) \tag{74}$$

2. *starting from inconsistent initial value* $\tilde{q}_k$ *such that* $\tilde{q}_k - q_k = \mathcal{O}(h^{p+1})$*, the error made by the RK method (73) is*

$$\tilde{q}_{k+1} - q_{k+1} = \mathcal{O}(h^{p+1}) \tag{75}$$

The assumption 5.1 is ensured by the result in [Hairer and Wanner, 1996, Theorem 1.1, Sec. IV.1]. The assumption 5.2 should be obtained by extending results of [Hairer et al., 1987] on the convergence of RK methods and the influence of perturbations. Rather than a long text explanation of an implementation of such a scheme, we propose to outline the main features of the method in Algorithm 1.

The local error on the whole time–step is given by the following theorem

Theorem 1 *Let us assume that Assumptions 1, 2 and 5 hold. The local error of consistency of the scheme described by Algorithm 1 has a local error of consistency of order p in the generalized coordinates that is*

$$e_q = \mathcal{O}(h^{p+1}). \tag{76}$$

proof If there is no event in the interval $I_k = [t_k, t_{k+1}]$, the result is trivial. Otherwise, the proof is given by induction on the finite sequence of the time intervals $[t_{k,i}, t_{k,i+1}]$ generated by Algorithm 1. Let us assume that the error by the scheme up to the time $t_{k,i}$ is

$$e_{k,i} = q_{k,i} - q(t_{k,i}) = \mathcal{O}(h^{p+1}) \tag{77}$$

We denote by $\tilde{q}_{k,i+1}$ and $\tilde{v}_{k,i+1}$ the values obtained by the time integration method on $[t_{k,i}, t_{k,i+1}]$ starting from the exact values $q(t_{k,i})$ and $v(t_{k,i})$. The time–integration on the time–interval $[t_{k,i}, t_{k,i+1}]$ is performed by one of the following scheme

1. *Moreau's time stepping scheme.* We have in this case that

$$e_{k,i+1} = q_{k,i+1} - q(t_{k,i+1}) = q_{k,i+1} - \tilde{q}_{k,i+1} + \tilde{q}_{k,i+1} - q(t_{k,i+1}). \tag{78}$$

   Thanks to Proposition 1, we get $q(t_{k,i+1}) - \tilde{q}_{k,i+1} = \mathcal{O}(\bar{h})$. For the remaining part of the error, we can write

$$\begin{array}{rcl} e_{k,i+1} & = & q_{k,i} + \bar{h}(\theta v_{k,i+1} + (1-\theta)v_{k,i}) - (q(t_{k,i}) + \bar{h}(\theta \tilde{v}_{k,i+1} + (1-\theta)\tilde{v}_{k,i})) + \mathcal{O}(\bar{h}), \\ & = & e_{k,i} + \bar{h}(\theta(v_{k,i+1} - \tilde{v}_{k,i+1}) + (1-\theta)(v_{k,i} - \tilde{v}_{k,i})) + \mathcal{O}(\bar{h}), \\ & = & \mathcal{O}(h^{p+1}) + \mathcal{O}(\bar{h}) = \mathcal{O}(h^{p+1}). \end{array} \tag{79}$$

2. *Index-1 DAE solver (73).* We have in this case that

$$e_{k,i+1} = q_{k,i+1} - q(t_{k,i+1}) = q_{k,i+1} - \tilde{q}_{k,i+1} + \tilde{q}_{k,i+1} - q(t_{k,i+1}). \tag{80}$$

   Using Assumption 5, we obtain $e_{k,i+1} = \mathcal{O}(h^{p+1})$.

By induction of the finite number of time–interval inside $[t_k, t_{k+1}]$ the result is obtained. □

6.2 Numerical applications

Theorem 1 is illustrated on the benchmark Example 1 and 2 on Figure 6 for standard implicit RK methods. The implicit RK methods are the well-known RADAU IIA methods of order 3 and 5 and Lobatto IIIA methods of order 2, 4 and 6. Details on these methods can be found in [Hairer et al., 1993, Hairer and Wanner, 1996]. Similar results for half–explicit RK methods can be found in Figure 7.

Figure 6 presents the global error in generalized coordinates with respect to the time–step. The conclusion are quite encouraging since we retrieve the global order of the associated RK methods even in presence of finite accumulation of impacts.

Algorithm 1 Higher order event–capturing time–stepping scheme for the step k.

Require: DAE solver of order p for the smooth index-1 dynamics with bilateral constraints (71).
Require: h time–step, $I = [t_k, t_{k+1}]$
Require: q_k, v_k initial conditions of the step.
Require: $C \in \mathbb{R}_+$, user defined positive constant
  // Initialization
  $i \leftarrow 0$
  $I_{k,i} \leftarrow [t_k, t_{k+1}], t_{k,i} \leftarrow t_k, t_{k,N} \leftarrow t_{k+1}$
  $q_{k,i} \leftarrow q_k, v_{k,i} \leftarrow v_k$
  Compute $\mathcal{I}_{k,i} = \{\alpha \in 1 \dots m \mid g^\alpha(g(q_{k,i})) \leqslant 0\}$ the index set of active constraints at time $t_{k,i}$
  // Integration
  while $t_{k,i} < t_{k+1}$ **do**
    Compute q_{k+1}, v_{k+1} by the integration over I_i the system (71) with the DAE solver of order p and a constant index set $\mathcal{I}_i$
    Compute $\mathcal{I}_{k+1} = \{\alpha \in 1 \dots m \mid g^\alpha(g(q_{k+1})) \leqslant 0\}$
    if $\mathcal{I}_i \neq \mathcal{I}_{k+1}$ **then**
      Locate roughly the first event time $t_{i,*}$ such that

$$t_{i,*} \in [t_{k,i+1}, t_{k,i+2}], \quad |t_{k,i+2} - t_{k,i+1}| \leqslant Ch^{p+1}, t_{k,i+2} \leqslant t_{k+1}$$

      // Smooth time integration
      Compute $q_{k,i+1}, v_{k,i+1}$ by the integration over $[t_{k,i}, t_{k,i+1}]$ the system (71) with the DAE solver of order p and a constant $\mathcal{I}_i$
      // Nonsmooth time integration
      Compute $q_{k,i+2}, v_{k,i+2}$ by the integration over $[t_{k,i+1}, t_{k,i+2}]$ the system (13) with Moreau's time stepping scheme
      $i \leftarrow i + 2$
      Update $\mathcal{I}_{k,i} = \{\alpha \in 1 \dots m \mid g^\alpha(g(q_{k,i})) \leqslant 0\}$
      $I_i \leftarrow [t_{k,i}, t_{k+1}]$
    end if
  end while

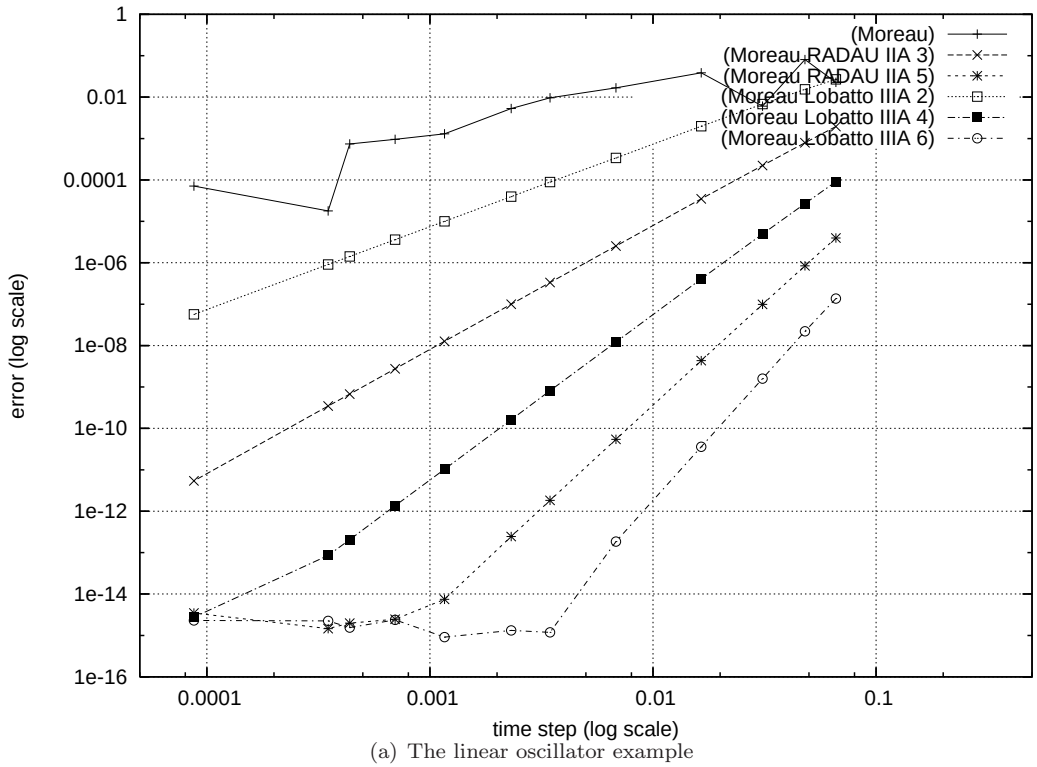

(a) The linear oscillator example

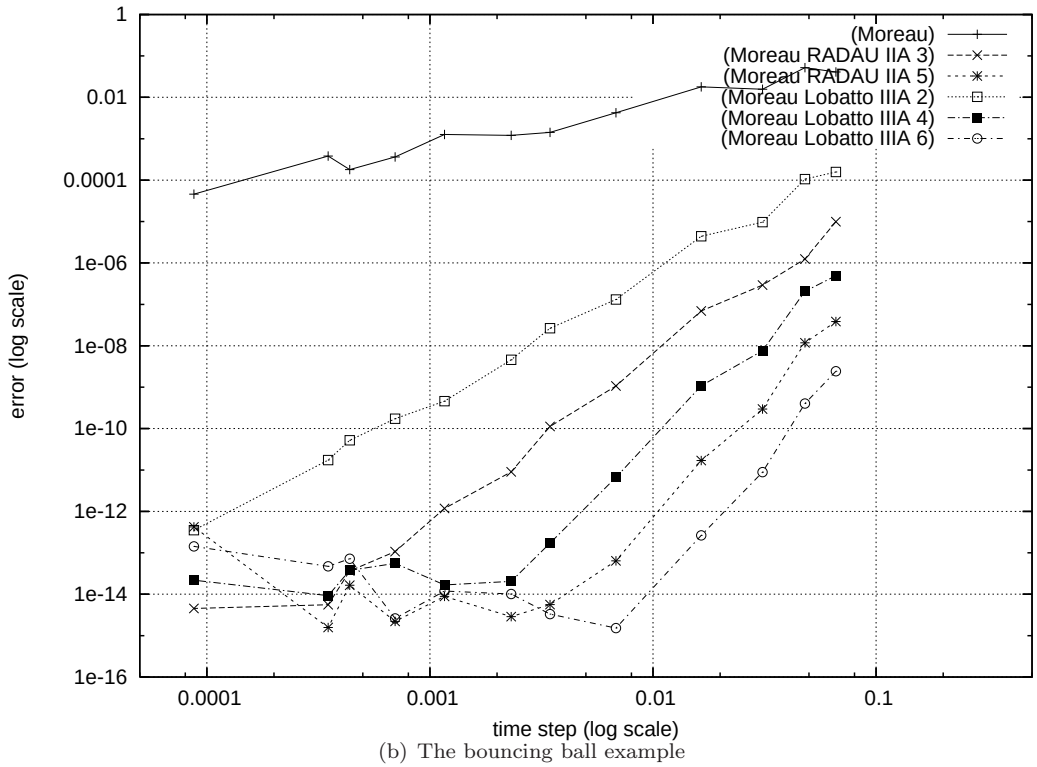

(b) The bouncing ball example

Figure 6: Order of accuracy. Implicit Runge–Kutta methods coupled with Moreau's time–stepping scheme.

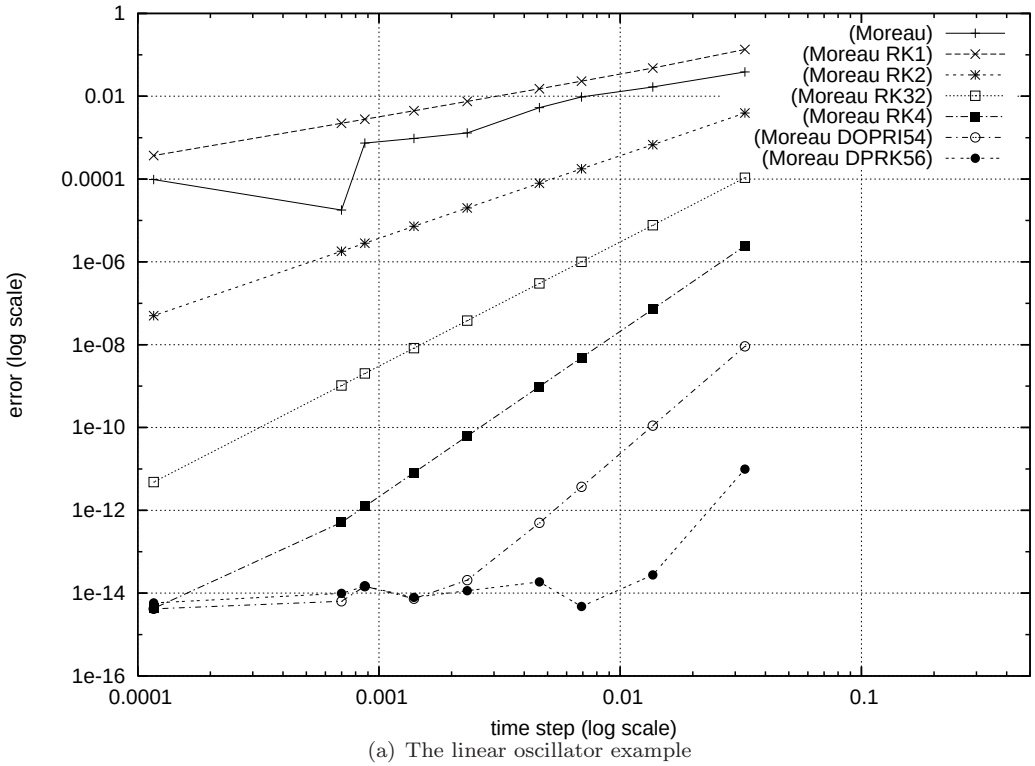

(a) The linear oscillator example

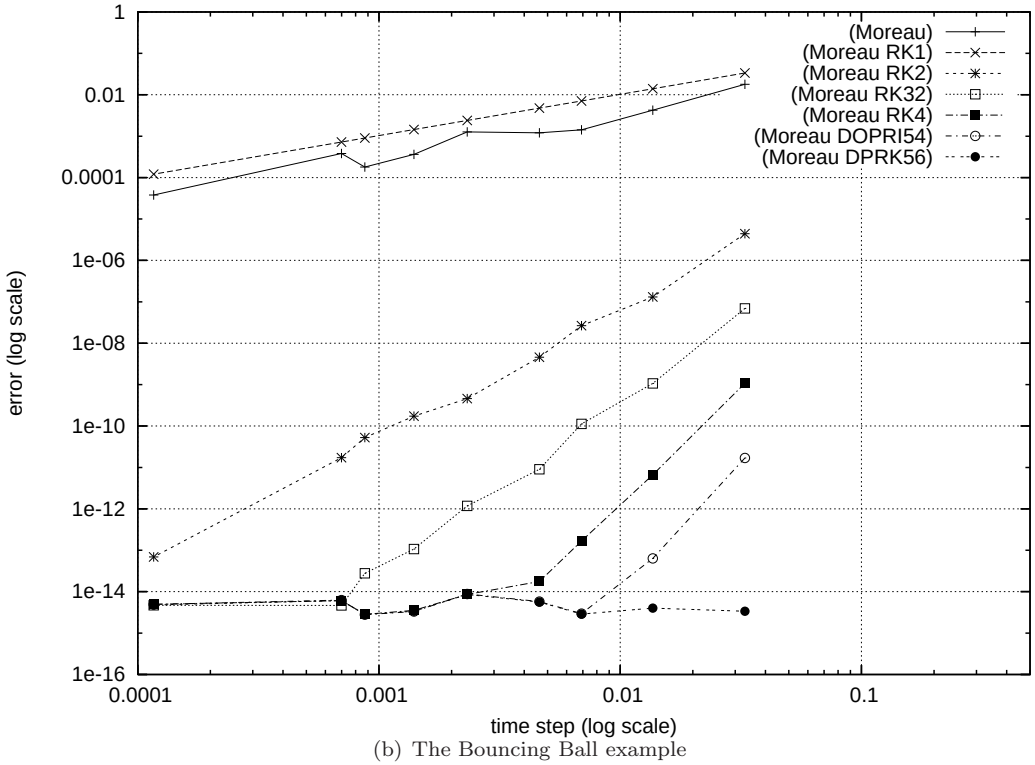

(b) The Bouncing Ball example

Figure 7: Order of accuracy. Half-Explicit Runge–Kutta methods coupled with Moreau's time–stepping scheme.

7 Conclusions and perspectives

In this paper, several approaches have been proposed to improve the resolution (ratio computational cost /error) and the order of accuracy of the Moreau time–stepping scheme. As far as we know, the results on the order of consistency of the Moreau time–stepping scheme are original. Unfortunately, the estimates on the accuracy of the method which are very low and attained on very simple examples do not allow the use of sophisticated variable time–step strategies. This is one of the main motivations to design higher order event–capturing schemes. A first attempt to build such a scheme is proposed in this paper by coupling standard Runge–Kutta scheme for DAE with the Moreau's scheme. This new scheme behaves well on simple academic examples and has to be improved on more complex nonlinear multibody systems.

The perspectives for this work are to improve the theoretical framework for such type of schemes. For instance, Assumption 5 should be improved or proved by standard arguments. The use of index-2 DAE form in smooth phases should also be considered together with the possible study of order reduction due to propagation of error in the multiplier [Arnold, 1995, 2008]. The case of Coulomb's friction should be also treated with the same kind of methods. Finally, the main open issue for higher order time–stepping scheme is to prove if the global error can be extrapolated in order to use standard but enhanced adaptive time–step strategies.

Acknowledgements

This work has been supported by the French National Research Agency (ANR) trough COSINUS program (project SALADYN ANR-08-COSI-014)`http://saladyn.inria.gforge.fr/`.

References

M. Abadie. Dynamic simulation of rigid bodies: Modelling of frictional contact. In B. Brogliato, editor, *Impacts in Mechanical Systems: Analysis and Modelling*, volume 551 of *Lecture Notes in Physics (LNP)*, pages 61–144. Springer, 2000.

V. Acary and B. Brogliato. *Numerical Methods for Nonsmooth Dynamical Systems: Applications in Mechanics and Electronics*, volume 35 of *Lecture Notes in Applied and Computational Mechanics*. Springer Verlag, http://www.springer.com/france/home/generic/search/results?SGWID=7-40109-22-173762912-0, 2008.

V. Acary, C.I. Morarescu, F. Pérignon, and B. Brogliato. Numerical simulation of nonsmooth systems and switching control with the siconos/control toolbox. In *6th Euromech Nonlinear Dynamics Conference, ENOC 2008,*, St Petersburg., 29 June 2008.

M. Arnold. A perturbation analysis for the dynamical simulation of mechanical multibody systems. *Appl. Numer. Math.*, 18:37–56, 1995.

M. Arnold. Numerical methods for simulation in applied dynamics. In Arnold and Schiehlen [2008], pages 191–246.

M. Arnold and W. Schiehlen, editors. *Simulation Techniques in Applied Dynamics*, volume 507 of *CISM Courses and Lectures*, 2008. Springer.

P. Ballard. The dynamics of discrete mechanical systems with perfect unilateral constraints. *Archives for Rational Mechanics and Analysis*, 154:199–274, 2000.

P. Ballard. Bounded variations and measure theory on the line. Lectures notes of the second summer on Nonsmooth Dynamics held in Autrans (France), 2003.

K.E. Brenan, S. Campbell, and L.R. Petzold. *Numerical Solution of Initial-Value Problems in Differential-Algebraic Equations*. North-holland, 1989.

B. Brogliato. *Nonsmooth Mechanics: Models, Dynamics and Control*. Springer-Verlag, London, 2nd edition, 1999.

O. Brüls, A. Cardona, and M. Géradin. Modeling, simulation and control of flexible multibody systems. In Arnold and Schiehlen [2008], pages 21–74.

R. Dzonou and M.D.P. Monteiro Marques. A sweeping process approach to inelastic contact problems with general inertia operators. *European Journal of Mechanics A/Solids*, 26(3):474–490, 2007.

C.W. Gear, B. Leimkuhler, and G.K. Gupta. Automatic integration of Euler-Lagrange equations with constraints. *Journal of Computational and Applied Mathematics*, 12–13:77–90, 1985.

Ch. Glocker, E. Cataldi-Spinola, and R.I. Leine. Curve squealing of trains: Measurement, modelling and simulation. *Journal of Sound and Vibration*, 324(1–2):365–386, 2009.

M. Géradin and A. Cardona. *Flexible Multibody Dynamics: A finite element Approach*. J. Wiley & Sons, New York, 2001.

E. Hairer and G. Wanner. *Solving Ordinary Differential Equations II. Stiff and Differential-Algebraic Problems.* Springer, 1996.

E. Hairer, Ch. Lubich, and M. Roche. *The Numerical Solution of Differential–Algebraic Systems by Runge–Kutta Methods*. Springer–Verlag, 1987.

E. Hairer, S.P. Norsett, and G. Wanner. *Solving Ordinary Differential Equations I. Nonstiff Problems.* Springer, 1993.

Andrei Herdt, Holger Diedam, Pierre-Brice Wieber, Dimitar Dimitrov, Katja Mombaur, and Moritz Diehl. Online Walking Motion Generation with Automatic Foot Step Placement (under review). *Advanced Robotics*, 2009. URL `http://hal.inria.fr/inria-00391408/en/`.

O. Janin and C.H. Lamarque. Comparison of several numerical methods for mechanical systems with impacts. *Int. J. Numer. Methods Eng.*, 51(9):1101–1132, 2001.

P. Lötstedt and L.R. Petzold. Numerical solution of nonlinear algebraic equations with algebraic constraints: I - convergence results for backward differentation formulas. *Mathematics of Computation*, 46(174):491–516, 1986.

M. Mabrouk. A unified variational for the dynamics of perfect unilateral constraints. *European Journal of Mechanics - A/Solids*, 17:819–842, 1998.

R. Mannshardt. One-step methods of any order for ordinary differential equations with discontinuous right-hand sides. *Numerische Mathematik*, 31:131–152, 1978.

M.D.P. Monteiro Marques. *Differential Inclusions in Nonsmooth Mechanical Problems. Shocks and Dry Friction.* Progress in Nonlinear Differential Equations and their Applications, vol.9. Birkhauser, Basel, 1993.

Jean Jacques Moreau. Approximation en graphe d'une évolution discontinue. *RAIRO, Anal. Numér.*, 12:75–84, 1978.

J.J. Moreau. Liaisons unilatérales sans frottement et chocs inélastiques. *Comptes Rendus de l'Académie des Sciences*, 296 série II:1473–1476, 1983.

J.J. Moreau. Unilateral contact and dry friction in finite freedom dynamics. In J.J. Moreau and Panagiotopoulos P.D., editors, *Nonsmooth Mechanics and Applications*, number 302 in CISM, Courses and lectures, pages 1–82. CISM 302, Spinger Verlag, Wien- New York, 1988a.

J.J. Moreau. Bounded variation in time. In J.J Moreau, P.D. Panagiotopoulos, and G. Strang, editors, *Topics in Nonsmooth Mechanics*, pages 1–74, Basel, 1988b. Bikhuser.

J.J. Moreau. Numerical aspects of the sweeping process. *Computer Methods in Applied Mechanics and Engineering*, 177:329–349, 1999. Special issue on computational modeling of contact and friction, J.A.C. Martins and A. Klarbring, editors.

J.J. Moreau. *Fonctionnelles Convexes.* Séminaire sur les équations aux dérivées partielles, subventionné par le CNRS, Collège de France, Paris., 1967.

L. Paoli. An existence result for non-smooth vibro-impact problems. *Journal of Differential Equations*, 211:247–281, 2005.

L. Paoli and M. Schatzman. A numerical scheme for impact problems I: The one-dimensional case. *SIAM Journal of Numerical Analysis*, 40(2):702–733, 2002a.

L. Paoli and M. Schatzman. A numerical scheme for impact problems II: The multi-dimensional case. *SIAM Journal of Numerical Analysis*, 40(2):734–768, 2002b.

L. Paoli and M. Schatzman. Approximation and existence in vibro-impact. *Comptes Rendus de l'Académie des Sciences*, 329, Série I:1103–1107, 1999.

F. Pfeiffer and C. Glocker. *Multibody Dynamics with Unilateral Contacts.* Non-linear Dynamics. John Wiley & Sons, 1996.

R.T. Rockafellar. *Convex Analysis.* Princeton University Press, 1970.

M. Schatzman. A class of nonlinear differential equations of second order in time. *Nonlinear Analysis, T.M.A*, 2(3):355–373, 1978.

D. Stewart. Convergence of a time-stepping scheme for rigid-body dynamics and resolution of Painlevé's problem. *Archives for Rational Mechanics and Analysis*, 145:215–260, 1998.

D. Stewart. Rigid body dynamics with friction and impact. *S.I.A.M. Review*, 42(1):3–39, 2000.

C. Studer. *Numerics of Unilateral Contacts and Friction. – Modeling and Numerical Time Integration in Non-Smooth Dynamics*, volume 47 of *Lecture Notes in Applied and Computational Mechanics*. Springer Verlag, 2009.

C. Studer, R. I. Leine, and Ch. Glocker. Step size adjustment and extrapolation for time stepping schemes in non-smooth dynamics. *International Journal for Numerical Methods in Engineering*, 76(11):1747–1781, 2008.

Contents

Centre de recherche INRIA Grenoble – Rhône-Alpes
655, avenue de l'Europe - 38334 Montbonnot Saint-Ismier (France)

Centre de recherche INRIA Bordeaux – Sud Ouest : Domaine Universitaire - 351, cours de la Libération - 33405 Talence Cedex
Centre de recherche INRIA Lille – Nord Europe : Parc Scientifique de la Haute Borne - 40, avenue Halley - 59650 Villeneuve d'Ascq
Centre de recherche INRIA Nancy – Grand Est : LORIA, Technopôle de Nancy-Brabois - Campus scientifique
615, rue du Jardin Botanique - BP 101 - 54602 Villers-lès-Nancy Cedex
Centre de recherche INRIA Paris – Rocquencourt : Domaine de Voluceau - Rocquencourt - BP 105 - 78153 Le Chesnay Cedex
Centre de recherche INRIA Rennes – Bretagne Atlantique : IRISA, Campus universitaire de Beaulieu - 35042 Rennes Cedex
Centre de recherche INRIA Saclay – Île-de-France : Parc Orsay Université - ZAC des Vignes : 4, rue Jacques Monod - 91893 Orsay Cedex
Centre de recherche INRIA Sophia Antipolis – Méditerranée : 2004, route des Lucioles - BP 93 - 06902 Sophia Antipolis Cedex

Éditeur
INRIA - Domaine de Voluceau - Rocquencourt, BP 105 - 78153 Le Chesnay Cedex (France)
http://www.inria.fr
ISSN 0249-6399